J Appl Electrochem (2009) 39:391–402
DOI 10.1007/s10800-008-9684-2

ORIGINAL PAPER

# Role of some thiadiazole derivatives as inhibitors for the corrosion of C-steel in 1 M $H_2SO_4$

**A. S. Fouda · F. E. Heakal · M. S. Radwan**

Received: 17 January 2008 / Accepted: 3 October 2008 / Published online: 11 December 2008


**Abstract** Inhibition of C-steel corrosion by some thiadiazole derivatives (I–VI) in 1 M $H_2SO_4$ was investigated by weight loss, potentiodynamic polarization, linear polarization resistance (LPR) and electrochemical impedance spectroscopy (EIS) techniques. The presence of these compounds in the solution decreases the double layer capacitance, increases the charge transfer resistance and increase of linear polarization. Polarization studies were carried out at room temperature, and showed that all the compounds studied are mixed type inhibitors with a slight predominance of cathodic character. The effect of temperature on corrosion inhibition has been studied and the thermodynamic activation and adsorption parameters were calculated and discussed. Electrochemical impedance was used to investigate the mechanism of corrosion inhibition. The adsorption of the compounds on C-steel was found to obey Langmuir's adsorption isotherm. The synergistic effect brought about by combination of the inhibitors and KSCN, KI and KBr was examined and explained. The mechanism of inhibition process was discussed in the light of the chemical structure and quantum-chemical calculations of the investigated inhibitors.

**Keywords** Thiadiazole derivatives · Corrosion · C-steel · $H_2SO_4$ · Quantum chemical calculation

A. S. Fouda (✉)
Department of Chemistry, Faculty of Science, El-Mansoura University, El-Mansoura 35516, Egypt
e-mail: asfouda@hotmail.com; asfouda@mans.edu.eg

F. E. Heakal
Department of Chemistry, Faculty of Science, Cairo University, Geza, Egypt

M. S. Radwan
Petrogulf Misr Company, Maadi, Cairo, Egypt

## 1 Introduction

C-steel, the most widely used engineering material, accounts for approximately 85% of the annual steel production world wide. Despite its relatively limited corrosion resistance, C-steel is used in large tonnages in marine applications, chemical processing, petroleum production and refining, construction and metal-processing equipment. The use of chemical inhibitors to decrease the rate of corrosion processes of carbon steels is quite varied [1–5]. A variety of organic compounds containing heteroatoms such as O, N, S and multiple bonds in their molecule are of particular interest as they give better inhibition efficiency than those containing N or S alone [6, 7]. Sulfur and/or nitrogen containing heterocyclic compounds with various substituents are considered to be effective corrosion inhibitors. Thiadiazole derivatives offer special affinity to inhibit corrosion of metals in acid solutions [8–11].

The present work was designed to study the corrosion inhibition of C-steel in $H_2SO_4$ solutions by new thiadiazole derivatives as corrosion inhibitors using four different techniques: weight loss, potentiodynamic polarization, linear polarization and electrochemical impedance spectroscopy (EIS). The synergistic effect brought about by combination of the inhibitors with KSCN, KI and KBr was examined and explained. The effect of temperature on the corrosion behavior also was investigated.

## 2 Experimental techniques

1 M $H_2SO_4$ solution was prepared from an analytical reagent grade of $H_2SO_4$ 98% and bi-distilled water and was used as corrosive media in this study. All the experiments were performed at 298 ± 1 K with C-steel samples

containing (weight %): 0.200% C, 0.350% Mn, 0.024% P, 0.003% Si and the remainder iron. The inhibitors were synthesized in the laboratory according to a previously described experimental procedure [12] purified and characterized by NMR and IR spectroscopies and element analysis before use. The structure formula of the inhibitors examined is given in Fig. 1.

### 2.1 Weight loss method

C-steel specimens of dimensions $2 \times 2 \times 0.2$ cm, in triplicate, were mechanically polished successively with different grades emery papers, up to 1,200 grade, degreased in acetone rinsed with bi-distilled water and finally dried then immersed in 100 mL of 1 M $H_2SO_4$ solutions containing various concentrations of the inhibitors. The weight of the specimens before and after immersion was determined. The weight loss was used to calculate the percentage inhibition efficiency (% IE) using the equation:

$$\%\,\mathrm{IE} = \frac{W - W'}{W} \times 100 \tag{1}$$

where $W$ and $W'$ are the corrosion rates (mg $cm^{-2}$ $min^{-1}$) of carbon steel in 1 M $H_2SO_4$ in the absence and presence of different concentrations of inhibitors, respectively.

### 2.2 Potentiodynamic polarization method

Electrochemical polarization experiments were carried out in a glass cell with a capacity of 250 mL. A platinum electrode and a saturated calomel electrode (SCE) were used as a counter electrode and a reference electrode, respectively. The working electrode was in the form of a disc with an exposed area of 0.12 $cm^2$ that was cut from C-steel under investigation. A time interval of about 30 min was given for the system to attain a steady state and the open circuit potential (OCP) was noted. Both cathodic and anodic potentiodynamic polarization curves were recorded at 300 mV ± OCP and scan rate of 2 mV $s^{-1}$ using potentiostat-galvanostat Wenking model-PGS95 and a LINSEIS model Ly 1600-IIXYt recorder.

% IE was calculated using the equation:

$$\%\,\mathrm{IE} = \frac{i_{\mathrm{corr}} - i'_{\mathrm{corr}}}{i_{\mathrm{corr}}} \times 100 \tag{2}$$

where $i_{corr}$ and $i'_{corr}$ are the corrosion current densities in the absence and presence of the inhibitors, respectively.

### 2.3 Linear polarization resistance method

Polarization was done in the range of 25 mV ± OCP at a scan rate of 2 mV $s^{-1}$ and the slope of the linear segment was obtained as polarization resistance, $R_p$.

The % IE is evaluated as follow:

$$\%\,\mathrm{IE} = \frac{R'_{\mathrm{p}} - R_{\mathrm{p}}}{R'_{\mathrm{p}}} \times 100 \tag{3}$$

where $R_p$ and $R'_p$ are the polarization resistance values in the absence and presence of the inhibitors, respectively.

### 2.4 Electrochemical impedance spectroscopy (EIS)

EIS experiments were conducted at 298 ± 1 K at the OCP over a frequency range of 1 kHz to 1 Hz, with a signal amplitude perturbation of 10 mV using IM6e system (Zahner Elektrik, Germany) and personal computer. Nyquist plots were obtained from the results of these experiments. Values of the charge transfer resistance ($R_{ct}$) were obtained from these plots by determining the difference in the values of impedance at low and high frequencies, as suggested by Tsuru et al. [13].Values of the double layer capacitance ($C_{dl}$) were calculated from the frequency at which the impedance imaginary component ($-Z''$) was maximum, using the following equation:

$$f\left(-Z''_{\max}\right) = \frac{1}{2\pi C_{\mathrm{d1}} R_{\mathrm{ct}}} \tag{4}$$

% IE was calculated using the equation:

$$\%\,\mathrm{IE} = \frac{\left(1/R'_{\mathrm{ct}}\right) - \left(1/R_{\mathrm{ct}}\right)}{\left(1/R'_{\mathrm{ct}}\right)} \times 100 \tag{5}$$

where $R'_{ct}$ and $R_{ct}$ are the charge transfer resistance values in the absence and presence of the inhibitors, respectively.

## 3 Results

### 3.1 Weight loss

Weight loss of C-steel, in mg $cm^{-2}$ of the surface area, was determined at various time intervals in the absence and presence of different concentrations ($1 \times 10^{-6}$–$20 \times 10^{-6}$ M) of the thiadiazole derivatives (I–VI). The curves obtained in the presence of different concentrations of inhibitors fall significantly below that of free acid. Similar behaviors were obtained for the other inhibitors. Values of % IE are tabulated in Table 1. In all cases, the increase in the inhibitor concentration was accompanied by a decrease in the weight loss and an increase in % IE. These results lead to the conclusion that, these compounds under investigation are fairly efficient as inhibitors for C-steel dissolution in $H_2SO_4$ solution. Careful inspection of these results showed that, at the same inhibitor concentration, the ranking of the inhibitors according to % IE is as follow: VI > V > IV > III > II > I.

**Fig. 1** The Chemical structure of the investigated thiadiazole derivatives

I) N-[4-phenyl-5-(p-tolylimino)-4,5-dihydro-1,3,4-thiadiazole-2-yl] benzamide

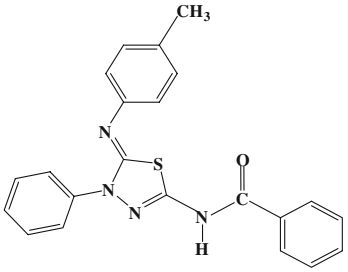

II) 2-acetyl-4-phenyl-5-(p-tolylimino)-4,5-dihydro-1,3,4-thiadiazole

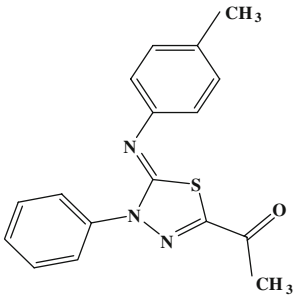

III) Ethyl-4-phenyl-5-(p-tolylimino)-4,5-dihydro-1,3,4-thiadiazole-2-carboxylate

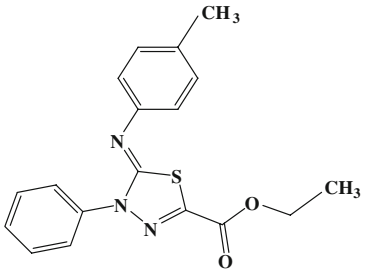

IV) 2-benzoyl-4-phenyl-5-(p-tolylimino)-4,5-dihydro-1,3,4-thiadiazole

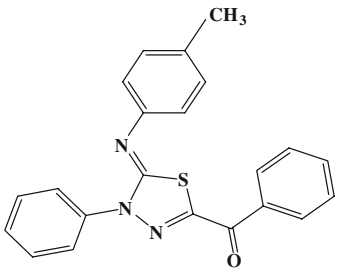

V) 2-benzoyl-4-phenyl-5-(4-bromophenylimino)-4,5-dihydro-1,3,4-thiadiazole

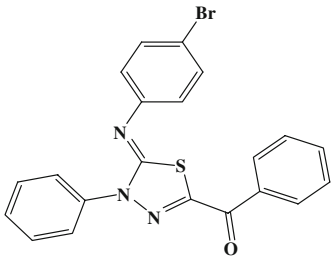

VI) 2-benzoyl-4-(p-tolyl)-5-(p-tolylimino)-4,5-dihydro-1,3,4-thiadiazole

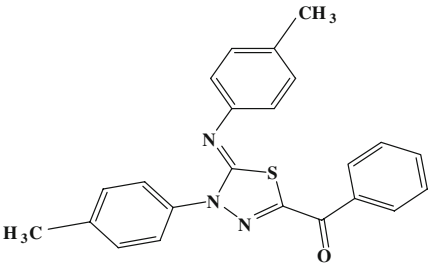

**Table 1** % IE of C-steel dissolution at 180 min immersion in 1 M $H_2SO_4$ in the presence of different concentrations of compounds (I–VI) at 298 K

| Conc. × $10^6$/M | I | II | III | IV | V | VI |
|---|---|---|---|---|---|---|
| 1 | 11.5 | 16.6 | 17.4 | 22.4 | 26.3 | 33.7 |
| 3 | 21.0 | 31.3 | 31.6 | 32.0 | 36.3 | 39.8 |
| 5 | 30.7 | 44.3 | 44.5 | 45.7 | 46.9 | 52.8 |
| 7 | 33.9 | 48.2 | 49.5 | 49.7 | 54.4 | 56.3 |
| 9 | 51.4 | 55.8 | 58.7 | 62.5 | 64.4 | 66.5 |
| 11 | 56.4 | 57.9 | 62.8 | 65.3 | 68.3 | 70.5 |
| 15 | 60.7 | 63.5 | 65.8 | 69.8 | 72.0 | 73.6 |
| 20 | 62.8 | 68.0 | 70.0 | 72.0 | 74.3 | 77.4 |

The value of dissolution rate of C-steel in 1 M $H_2SO_4$ = 0.14 mg $cm^{-2}$ $min^{-1}$

### 3.1.1 Synergistic effect

The effect of addition $1 \times 10^{-2}$ M KSCN, KI and KBr on the corrosion rate of C-steel in the absence and presence of different concentrations of inhibitors (I–VI) in 1 M $H_2SO_4$ solutions was investigated using weight loss method. Results of % IE obtained are summarized in Table 2. It was observed from these results, these additives improved the % IE significantly, due to the stabilization of adsorbed halide ions by means of electrostatic interactions with the inhibitor, which leads to greater surface coverage [14]. The interactions of these additives with the inhibitor molecules can be described by introduction of the synergistic parameter ($S_\theta$) which is defined as [15]:

$$S_\theta = \frac{1-\theta_{1+2}}{1-\theta'_{1+2}} \tag{6}$$

where $\theta_{1+2} = (\theta_1 + \theta_2) - (\theta_1\theta_2)$; $\theta_1$ = the degree of surface coverage by the anions; $\theta_2$ = the degree of surface coverage by the cations; $\theta'_{1+2}$ = measured surface coverage by both anions and cations.

$S_\theta$ approaches 1 when no interaction between the inhibitor compounds exists, while $S_\theta > 1$ points to a synergistic effect. In the case of $S_\theta < 1$, the antagonistic interaction prevails.

Values of $S_\theta$ summarized in Table 3 are more than unity, suggesting that the phenomenon of synergism exists between the inhibitors and these additives used. Aramaki [16] has proposed two kinds of joint adsorption (competitive and cooperative) to explain the synergistic action observed between an anion and a cation [17]. For competitive adsorption or interference adsorption, the anion ($X^-$) and cation (inhibitor molecules in acid medium) are adsorbed at different sites on the electrode surface and for cooperative adsorption, the anion ($X^-$) is chemisorbed on the surface and the cation (inhibitor molecules) is adsorbed

**Table 2** % IE at different concentrations of inhibitors (I–VI) for C-steel at 180 min immersion in 1 M $H_2SO_4$ containing $10^{-2}$ M KSCN, KI and KBr at 298 K

| Additives | Conc. × $10^6$/M | I | II | III | IV | V | VI |
|---|---|---|---|---|---|---|---|
| KSCN | 0 | 36.4 | | | | | |
| | 1 | 50.7 | 50.9 | 51.0 | 52.2 | 52.4 | 52.8 |
| | 3 | 60.6 | 60.7 | 60.9 | 62.1 | 62.2 | 62.5 |
| | 5 | 69.8 | 70.1 | 70.3 | 71.3 | 71.5 | 71.7 |
| | 7 | 73.3 | 73.5 | 73.7 | 74.8 | 75.0 | 75.2 |
| | 9 | 91.4 | 91.6 | 91.7 | 92.6 | 92.9 | 93.1 |
| | 11 | 96.2 | 96.3 | 96.5 | 97.5 | 97.7 | 97.9 |
| KI | 0 | 35.1 | | | | | |
| | 1 | 50.3 | 50.5 | 50.9 | 51.8 | 52.1 | 52.4 |
| | 3 | 60.2 | 60.3 | 60.5 | 61.7 | 61.9 | 62.6 |
| | 5 | 69.3 | 69.7 | 70.1 | 70.9 | 71.1 | 71.3 |
| | 7 | 72.8 | 73.7 | 73.7 | 74.4 | 74.7 | 74.8 |
| | 9 | 90.8 | 91.1 | 91.4 | 92.2 | 92.6 | 92.7 |
| | 11 | 95.7 | 95.9 | 96.3 | 97.1 | 97.3 | 97.5 |
| KBr | 0 | 32.8 | | | | | |
| | 1 | 49.3 | 50.9 | 50.7 | 51.3 | 52.2 | 52.4 |
| | 3 | 59.2 | 59.9 | 60.3 | 60.7 | 61.1 | 61.5 |
| | 5 | 68.9 | 70.1 | 70.9 | 71.7 | 70.9 | 71.3 |
| | 7 | 72.9 | 73.7 | 70.1 | 74.8 | 80.3 | 80.7 |
| | 9 | 80.3 | 81.5 | 81.6 | 82.1 | 83.1 | 83.5 |
| | 11 | 84.7 | 85.3 | 85.5 | 85.8 | 86.2 | 86.6 |

**Table 3** Synergistic parameters ($S_\theta$) of $10^{-2}$ M KSCN, KI and KBr at different concentrations of compounds (I–VI) for C-steel in 1 M $H_2SO_4$ at 298 K

| Additives | Conc. × $10^6$/M | I | II | III | IV | V | VI |
|---|---|---|---|---|---|---|---|
| KSCN | 1 | 1.14 | 1.10 | 1.08 | 1.04 | 0.99 | 0.90 |
| | 3 | 1.31 | 1.13 | 1.10 | 1.15 | 1.08 | 1.03 |
| | 5 | 1.47 | 1.19 | 1.17 | 1.19 | 1.12 | 1.07 |
| | 7 | 1.56 | 1.33 | 1.23 | 1.28 | 1.16 | 1.12 |
| | 9 | 3.44 | 4.02 | 3.25 | 3.38 | 3.29 | 3.00 |
| | 11 | 7.00 | 13.44 | 8.00 | 11.2 | 10.00 | 9.50 |
| KI | 1 | 1.14 | 1.12 | 1.10 | 1.06 | 1.00 | 0.90 |
| | 3 | 1.28 | 1.13 | 1.13 | 1.16 | 1.11 | 1.05 |
| | 5 | 1.45 | 1.20 | 1.17 | 1.21 | 1.17 | 1.03 |
| | 7 | 1.59 | 1.31 | 1.23 | 1.23 | 1.15 | 1.12 |
| | 9 | 3.54 | 3.22 | 2.89 | 3.00 | 3.29 | 3.00 |
| | 11 | 7.25 | 6.75 | 6.00 | 7.67 | 7.00 | 6.33 |
| KBr | 1 | 1.16 | 1.14 | 1.12 | 1.06 | 1.02 | 0.92 |
| | 3 | 1.29 | 1.15 | 1.13 | 1.15 | 1.10 | 1.05 |
| | 5 | 1.48 | 1.23 | 1.28 | 1.29 | 1.21 | 1.07 |
| | 7 | 1.63 | 1.35 | 1.14 | 1.32 | 1.55 | 1.53 |
| | 9 | 1.65 | 1.61 | 1.50 | 1.39 | 1.41 | 1.38 |
| | 11 | 1.93 | 1.87 | 1.79 | 1.64 | 1.50 | 1.46 |

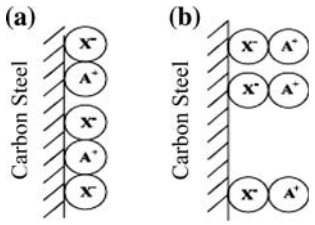


**Fig. 2** Schematic representations of **a** competitive and **b** cooperative adsorption of the anions ($X^-$) and cations ($A^+$) on carbon steel surface in acid solutions

on the layer of the anions. The two types of adsorption are represented schematically in Fig. 2 and can be characterized by a synergistic factor ($S_\theta$) calculated as above.

The synergistic inhibitive effect brought about by combination of the inhibitors with KSCN, KI and KBr for the corrosion of C-steel in 1 M $H_2SO_4$ can be explained as follows: The strong chemisorption of $X^-$ ions ($SCN^-$, $I^-$ or $Br^-$) on the metal surface is responsible for the synergistic effect of these anions, in attraction with protonated inhibitor [18]. $X^-$ ions are adsorbed on the anodic sites on the metal surface. Surface charge is changed to negative by the specific adsorption of these ions resulting in the joint adsorption of anions with the inhibitor cations. The inhibitors are believed to be adsorbable, not only on the cathodic sites by electrostatic attraction using the charge of the protonated molecule, but also on the anodic sites by virtue of donation of the electron-pair on the nitrogen atom of the unprotonated molecule [19] therefore, interference adsorption can take place at the anodic sites.

### 3.1.2 Adsorption isotherm

Attempts were made to fit the degree of surface coverage determined by weight loss ($\theta$) to various isotherms. The best fit was obtained with the Langmuir's isotherm which is in good agreement with Eq. 7 [20]. The variations of ($\theta$/ 1 − $\theta$) with the inhibitor concentrations (C) of compounds (I–VI) are represented in Fig. 3. According to the following equation:

$$\frac{\theta}{1-\theta} = K_{\text{ads}} \times C \tag{7}$$

where $K_{\text{ads}}$ is the equilibrium constant for the adsorption process, a linear relationship is obtained with slope equal to $K_{\text{ads}}$ which is related to the standard free energy of adsorption ($\Delta G^\circ_{\text{ads}}$) by the equation:

$$K_{\text{ads}} = \frac{1}{55.5}\exp\frac{-\Delta G^\circ_{\text{ads}}}{\text{RT}} \tag{8}$$

where 55.5 is the molar concentration of water in the solution, $R$ is the universal gas constant and $T$ is the absolute temperature.

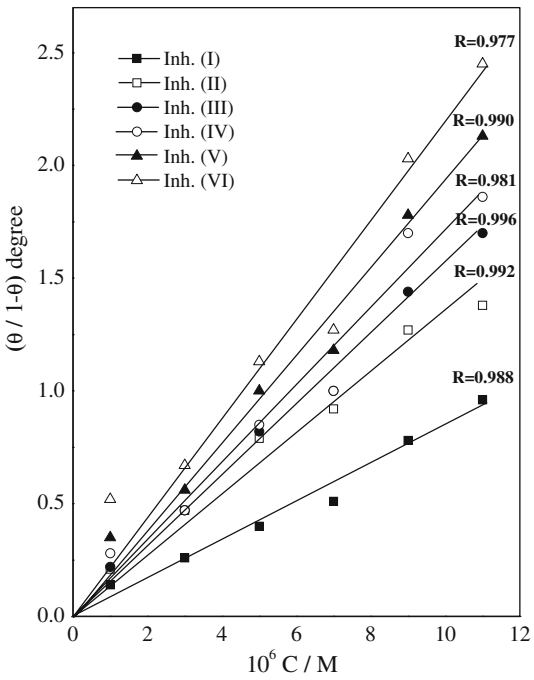


**Fig. 3** Langmuir adsorption isotherm for C-steel in 1 M $H_2SO_4$ in the presence of different concentrations of inhibitors (I–VI) at 298 K

cThe thermodynamic parameters for the adsorption process were obtained from these figures are shown in Table 4. The values of $\Delta G^\circ_{\text{ads}}$ are negative and increased as the % IE increased which indicate that these investigated compounds are strongly adsorbed on the C-steel surface and show the spontaneity of the adsorption process and stability of the adsorbed layer on the C-steel surface. Generally, values of $\Delta G^\circ_{\text{ads}}$ up to −20 kJ $mol^{-1}$ are consistent with the electrostatic interaction between the charged molecules and the charged metal (physical adsorption) while those more negative than −40 kJ $mol^{-1}$ involve sharing or transfer of electrons from the inhibitor molecules to the metal surface to form a coordinate type of bond (chemisorption) [21]. The values of $\Delta G^\circ_{\text{ads}}$ obtained were approximately equal to $-39 \pm 1$ kJ $mol^{-1}$, indicating that the adsorption mechanism of the thiadiazole derivatives on C-steel in 1 M $H_2SO_4$ solution involves both electrostatic adsorption and chemisorption [22]. The $K_{\text{ads}}$ follows the same trend in the sense that large values of $K_{\text{ads}}$ imply better more efficient adsorption and hence better inhibition efficiency [23].

### 3.1.3 Effect of temperature

Corrosion reactions are usually regarded as Arrhenius processes and the rate ($k$) can be expressed by the relation:

$$\log k = A - \frac{E_a}{2.303\,\text{RT}} \tag{9}$$

where $E_a$ is the activation energy of the corrosion process and $A$ is a Arrhenius pre-exponential constant depends on

**Table 4** Thermodynamic parameters of the adsorption of compounds (I–VI) on C-steel surface in 1 M $H_2SO_4$ at 298 K

| Inhibitor | $K_{ads}$/mol | $-\Delta G^{\circ}_{ads}$/kJ mol$^{-1}$ |
|---|---|---|
| I | 085,292 | 38.08 |
| II | 136,712 | 39.25 |
| III | 152,210 | 39.52 |
| IV | 171,704 | 39.81 |
| V | 194,620 | 40.13 |
| VI | 217,536 | 40.40 |

the metal type and electrolyte. Arrhenius plots of log $k$ vs. $1/T$ for carbon steel in 1 M $H_2SO_4$ in the absence and presence of 11 $\times$ $10^{-6}$ M of inhibitors (I–VI) are shown graphically in Fig. 4. The variation of log $k$ vs. $1/T$ is a linear one and the values of $E_a$ obtained are summarized in Table 5. These results show that the values of $E_a$ are similar and ranging from 61.34 to 68.40 kJ/mol suggest that the inhibitors are similar in the mechanism of action. The increase in $E_a$ with the addition of 11 $\times$ $10^{-6}$ M of inhibitors (I–VI) indicating that the energy barrier for the corrosion reaction increases. It is also indicated that the whole process is controlled by surface reaction, since the activation energy of the corrosion process is over 20 kJ/mol [24].

Enthalpy and entropy of activation ($\Delta H^*$, $\Delta S^*$) are calculated from transition state theory using the following equation [25]:

**Table 5** Activation parameters of carbon steel dissolution in 1 M $H_2SO_4$ in the absence and presence of 11 $\times$ $10^{-6}$ M of compounds (I–VI)

| Inhibitors | $E_a$/kJ mol$^{-1}$ | $\Delta H^*$/kJ mol$^{-1}$ | $-\Delta S^*$/J mol$^{-1}$ K$^{-1}$ |
|---|---|---|---|
| 1 M $H_2SO_4$ | 46.17 | 41.17 | 180.59 |
| I | 61.34 | 60.51 | 115.48 |
| II | 63.90 | 61.65 | 112.79 |
| III | 66.39 | 63.34 | 107.24 |
| IV | 67.16 | 64.33 | 104.75 |
| V | 67.75 | 65.48 | 101.88 |
| VI | 68.40 | 65.87 | 101.11 |

$$k = \frac{RT}{Nh}\exp\left(\frac{\Delta S^*}{R}\right)\exp\left(\frac{-\Delta H^*}{RT}\right) \quad (10)$$

where $h$ is Planck's constant, $N$ is Avogadro's number. A plot of log $k/T$ vs. $1/T$ also gave straight lines as shown in Fig. 5 for carbon steel dissolution in 1 M $H_2SO_4$ in the absence and presence of 11 $\times$ $10^{-6}$ M of inhibitors (I–VI). The slopes of these lines equal $-(\Delta H^*/2.303R$ and the intercept equal log $RT/Nh + (\Delta S^*/2.303R)$ from which the value of $\Delta H^*$ and $\Delta S^*$ were calculated and tabulated in Table 5. From these results, it is clear that the presence of the tested compounds increased the activation energy values and consequently decreased the corrosion rate of the carbon steel. These results indicate that these tested compounds

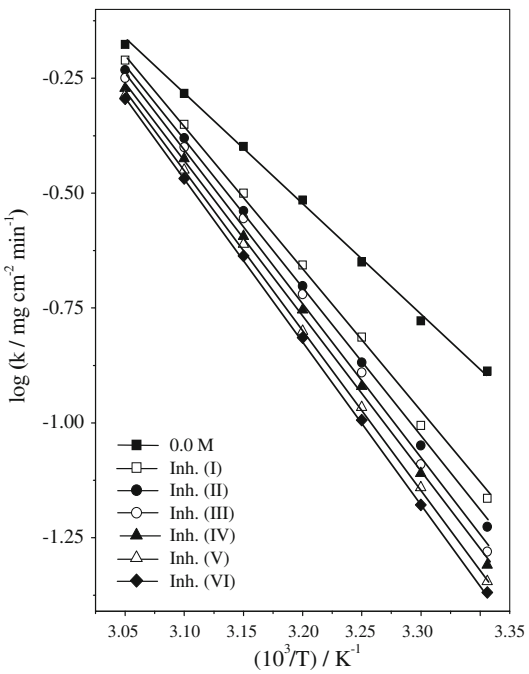


**Fig. 4** Log $k$ – $1/T$ plots for carbon steel dissolution in 1 M $H_2SO_4$ in the absence and presence of 11 $\times$ $10^{-6}$ M of inhibitors (I–VI)

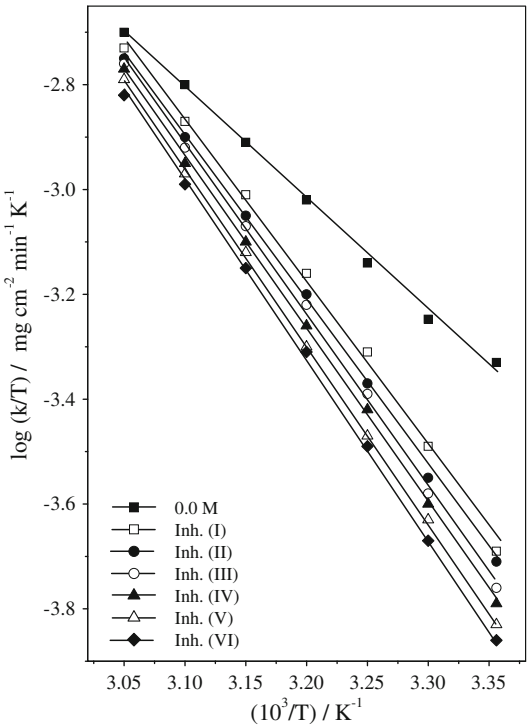


**Fig. 5** Log $(k/T)$–$(1/T)$ plots for carbon steel dissolution in 1 M $H_2SO_4$ in the absence and presence of 11 $\times$ $10^{-6}$ M of inhibitors (I–VI)

acted as inhibitors through increasing activation energy of carbon steel dissolution by making a barrier to mass and charge transfer by their adsorption on carbon steel surface. The values of $\Delta H^*$ reflect the strong adsorption of these compounds on carbon steel surface. The values of $\Delta S^*$ in absence and presence of the tested compounds are large and negative; this indicates that the activated complex in the rate-determining step represents an association rather than dissociation step, meaning that a decreases in disordering takes place on going from reactants to the activated complex and the activated molecules were in higher order state than that at the initial state [26, 27].

### 3.2 Potentiodynamic polarization

Anodic and cathodic polarization were carried out potentiodynamically in unstirred 1 M $H_2SO_4$ solution in the absence and presence of various concentrations of the inhibitors (I–VI) at 298 K over potential range 300 mV ± OCP. The results are represented in Fig. 6 for compound (VI), similar behaviors were obtained for other compounds. The obtained potentiodynamic polarization parameters are given in Table 6. These results indicate that the cathodic and anodic curves obtained exhibit Tafel-type behavior. Additionally, the form of these curves is very similar either in the cathodic or in the anodic side, which indicates that the

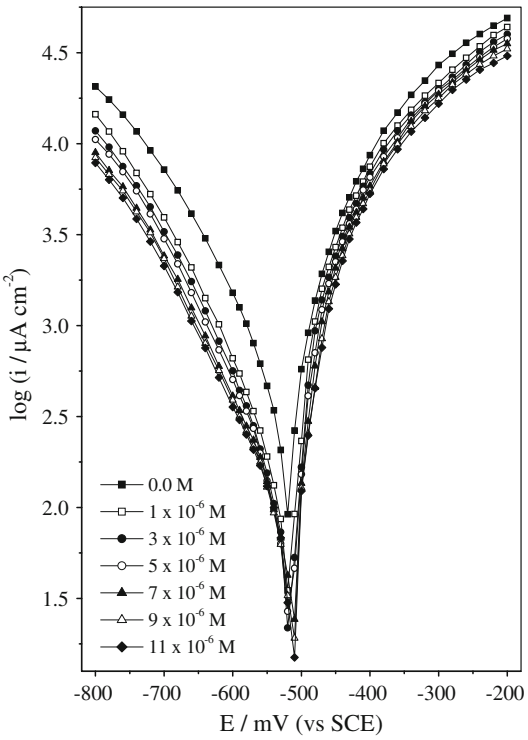


**Fig. 6** Potentiodynamic polarization curves for carbon steel in 1 M $H_2SO_4$ in the absence and presence of different concentrations of inhibitor (VI) at 298 K

mechanisms of carbon steel dissolution and hydrogen reduction apparently remain unaltered in the presence of these additives. Addition of thiadiazole derivatives decreased both the cathodic and anodic current densities and caused mainly parallel displacement to the more negative and positive values, respectively, i.e. the presence of thiadiazole derivatives in solution inhibits both the hydrogen evolution and the anodic dissolution processes with overall shift of $E_{corr}$ to more negative values with respect to the OCP.

The results also show that the anodic and cathodic Tafel slopes ($\beta_a$ and $\beta_c$) slightly changed on increasing the concentration of the tested compounds. This indicates that there is no change of the mechanism of inhibition in presence and absence of inhibitors. This could be interpreted as an action of mixed inhibitor control over the electrochemical semi-reactions. This means that the thiadiazole derivatives are mixed type inhibitors, but the cathode is more preferentially polarized than the anode. The higher values of Tafel slope can be attributed to surface kinetic process rather the diffusion-controlled process [28]. The constancy and the parallel of cathodic slope obtained from the electrochemical measurements indicate that the hydrogen evolution reaction was activation controlled [29] and the addition of these derivatives did not modify the mechanism of this process. This result suggests that the inhibition mode of the thiadiazole derivatives used was by simple blockage of the surface by adsorption.

### 3.3 Linear polarization resistance (LPR)

LPR values were obtained from current/potential plots. The obtained linear polarization plots for C-steel in 1 M $H_2SO_4$ in the absence and presence of different concentrations of compound (VI) is shown in Fig. 7, similar behaviors were obtained for other compounds. LPR parameters of different thiadiazole derivatives (I–VI) are given in Table 6. The slope of these curves ($R_p$) showed an increase values from 39.8 Ω cm$^2$ for the inhibitor free solution to 153.4 Ω cm$^2$ in the presence of 11 × $10^{-6}$ M of compound (VI). Also, the values of $R_p$, and consequently the % IE, increase with increasing the concentrations of the thiadiazole derivatives which indicates that these compounds act as inhibitors.

### 3.4 Electrochemical impedance spectroscopy

Impedance diagrams (Nyquist and Bode) at frequencies ranging from 1 Hz to 1 kHz with 10 mV amplitude signal at OCP for carbon steel in 1 M $H_2SO_4$ in the absence and presence of different concentrations of compounds (I–VI) are obtained. The equivalent circuit

**Table 6** Potentiodynamic polarization and LPR parameters for corrosion of carbon steel in 1 M $H_2SO_4$ in the absence and presence of different concentrations of inhibitors (I–VI) at 298 K

| Inhibitors | Conc. × $10^6$/M | $-E_{corr}$/mV | $i_{corr}$/μA cm$^{-2}$ | $\beta_c$/mV dec$^{-1}$ | $\beta_a$/mV dec$^{-1}$ | $R_p$/Ω cm$^2$ | % IE | |
|---|---|---|---|---|---|---|---|---|
| | | | | | | | Potentio. | LPR |
| Blank | 0 | 507 | 563 | 145 | 95 | 39.8 | – | – |
| I | 1 | 525 | 380 | 137 | 85 | 56.8 | 32.5 | 29.9 |
| | 3 | 531 | 363 | 135 | 85 | 61.4 | 36.0 | 35.1 |
| | 5 | 533 | 339 | 130 | 80 | 64.1 | 40.1 | 37.9 |
| | 7 | 535 | 275 | 130 | 82 | 77.5 | 50.9 | 48.6 |
| | 9 | 538 | 251 | 135 | 85 | 86.2 | 55.0 | 53.8 |
| | 11 | 540 | 224 | 137 | 87 | 100.0 | 60.3 | 60.2 |
| II | 1 | 527 | 372 | 139 | 85 | 57.5 | 34.5 | 30.7 |
| | 3 | 531 | 355 | 135 | 83 | 62.6 | 37.1 | 36.3 |
| | 5 | 535 | 331 | 137 | 87 | 67.1 | 42.0 | 40.6 |
| | 7 | 538 | 269 | 133 | 85 | 80.0 | 52.6 | 50.2 |
| | 9 | 540 | 235 | 140 | 83 | 92.5 | 58.2 | 57.0 |
| | 11 | 543 | 214 | 139 | 87 | 105.3 | 61.9 | 62.2 |
| III | 1 | 530 | 363 | 140 | 85 | 58.1 | 35.7 | 31.5 |
| | 3 | 535 | 347 | 138 | 84 | 65.4 | 39.0 | 39.1 |
| | 5 | 539 | 316 | 140 | 85 | 69.4 | 44.2 | 42.6 |
| | 7 | 541 | 251 | 140 | 84 | 86.2 | 55.8 | 53.8 |
| | 9 | 543 | 224 | 142 | 87 | 101.0 | 60.2 | 60.6 |
| | 11 | 545 | 204 | 141 | 86 | 117.7 | 64.0 | 66.1 |
| IV | 1 | 535 | 355 | 130 | 90 | 60.6 | 36.9 | 34.3 |
| | 3 | 542 | 331 | 133 | 85 | 66.7 | 40.7 | 40.3 |
| | 5 | 544 | 309 | 135 | 90 | 69.9 | 45.9 | 42.9 |
| | 7 | 545 | 234 | 135 | 90 | 89.3 | 58.2 | 55.4 |
| | 9 | 547 | 214 | 130 | 85 | 109.9 | 62.5 | 63.8 |
| | 11 | 548 | 191 | 135 | 87 | 122.0 | 66.1 | 67.3 |
| V | 1 | 540 | 345 | 133 | 85 | 62.5 | 38.3 | 36.3 |
| | 3 | 542 | 324 | 136 | 88 | 70.4 | 42.5 | 43.4 |
| | 5 | 542 | 302 | 137 | 85 | 74.6 | 46.2 | 46.6 |
| | 7 | 546 | 219 | 140 | 90 | 95.2 | 60.8 | 58.2 |
| | 9 | 550 | 209 | 140 | 87 | 114.9 | 63.2 | 65.3 |
| | 11 | 552 | 170 | 145 | 93 | 133.3 | 69.6 | 70.1 |
| VI | 1 | 540 | 331 | 139 | 95 | 64.9 | 40.3 | 38.7 |
| | 3 | 542 | 324 | 135 | 91 | 72.5 | 43.3 | 45.0 |
| | 5 | 545 | 282 | 135 | 91 | 80.7 | 50.1 | 50.6 |
| | 7 | 552 | 219 | 140 | 90 | 97.1 | 61.1 | 59.0 |
| | 9 | 555 | 195 | 143 | 95 | 123.5 | 65.5 | 67.7 |
| | 11 | 557 | 159 | 143 | 95 | 153.9 | 71.6 | 74.7 |

that describes our metal/electrolyte interface is shown in Fig. 8 where $R_s$, $R_{ct}$ and CPE refer to solution resistance, charge transfer resistance and constant phase element, respectively. EIS parameters and % IE were calculated and tabulated in Table 7. In order to correlate impedance and polarization methods, $i_{corr}$ values were obtained from polarization curves and Nyquist plots in the absence and presence of different concentrations of compounds (I–VI) using the Stern-Geary equation:

$$i_{corr} = \frac{\beta_a \beta_c}{2.303(\beta_a + \beta_c)R_{ct}} \quad (11)$$

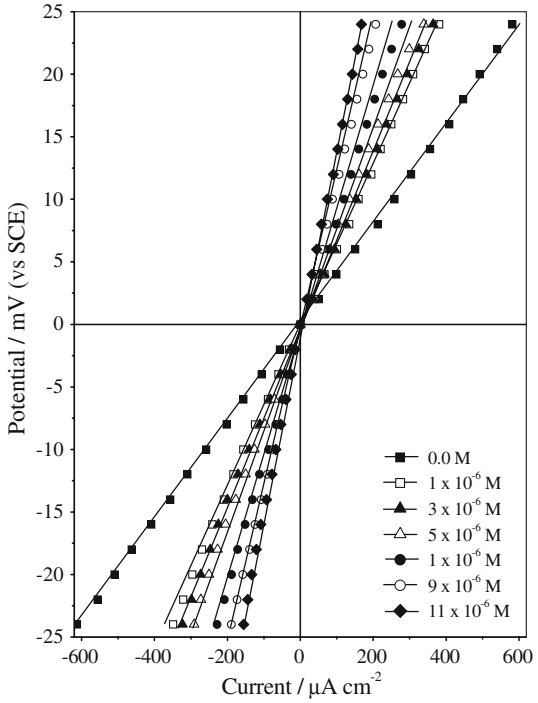


**Fig. 7** Linear polarization plots for carbon steel in 1 M $H_2SO_4$ in the absence and presence of different concentrations of inhibitor (VI) at 298 K

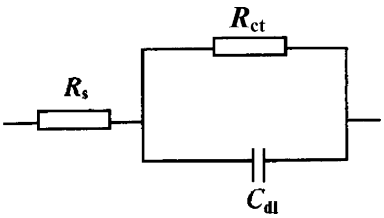


**Fig. 8** Equivalent circuit of constant phase element (CPE)

The obtained Nyquist plot for compound (VI) is shown in Fig. 9. Each spectrum is characterized by a single full semicircle. The fact that impedance diagrams have an approximately semicircular appearance shows that the corrosion of carbon steel is controlled by a charge transfer process. Small distortion was observed in some diagrams, this distortion has been attributed to frequency dispersion [30]. The diameters of the capacitive loop obtained increases in the presence of thiadiazole derivatives, and were indicative of the degree of inhibition of the corrosion process. The obtained Bode plot for compounds (VI) is shown in Fig. 10. The high frequency limits corresponds to $R_s$ (Ω), while the lower frequency limits corresponds to ($R_{ct} + R_s$). The low frequency contribution shows the kinetic response of the charge transfer reaction [31].

**Table 7** EIS Data for carbon steel in 1 M $H_2SO_4$ in the absence and presence of different concentrations of inhibitors (I–VI) at 298 K

| Inhibitors | Conc. × $10^6$/M | $R_{ct}$/Ω cm$^2$ | $C_{dl}$/μF cm$^{-2}$ | $i_{corr}$/μA cm$^{-2}$ | % IE |
|---|---|---|---|---|---|
| Blank | 0 | 31.17 | 29.33 | 801 | – |
| I | 1 | 46.32 | 20.73 | 492 | 32.7 |
| | 3 | 49.82 | 20.05 | 455 | 37.4 |
| | 7 | 62.71 | 17.54 | 349 | 50.3 |
| | 11 | 79.60 | 15.66 | 291 | 60.8 |
| II | 1 | 47.33 | 21.42 | 485 | 34.1 |
| | 3 | 51.89 | 20.05 | 442 | 39.9 |
| | 7 | 65.76 | 17.09 | 343 | 52.6 |
| | 11 | 94.38 | 15.81 | 247 | 66.9 |
| III | 1 | 48.45 | 20.70 | 481 | 35.7 |
| | 3 | 53.43 | 20.26 | 425 | 41.7 |
| | 7 | 67.66 | 17.47 | 337 | 53.9 |
| | 11 | 80.12 | 15.99 | 290 | 61.1 |
| IV | 1 | 48.49 | 23.67 | 477 | 35.7 |
| | 3 | 54.03 | 19.73 | 417 | 42.3 |
| | 7 | 73.52 | 16.23 | 319 | 57.6 |
| | 11 | 84.05 | 15.34 | 274 | 62.9 |
| V | 1 | 48.97 | 27.82 | 460 | 36.4 |
| | 3 | 57. 57 | 27.11 | 409 | 45.9 |
| | 7 | 77.12 | 17.04 | 309 | 59.6 |
| | 11 | 100.50 | 13.88 | 246 | 69.0 |
| VI | 1 | 54.85 | 19.67 | 447 | 43.2 |
| | 3 | 57.63 | 19.17 | 409 | 45.9 |
| | 7 | 77.20 | 15.97 | 309 | 59.6 |
| | 11 | 101.40 | 13.23 | 245 | 69.3 |

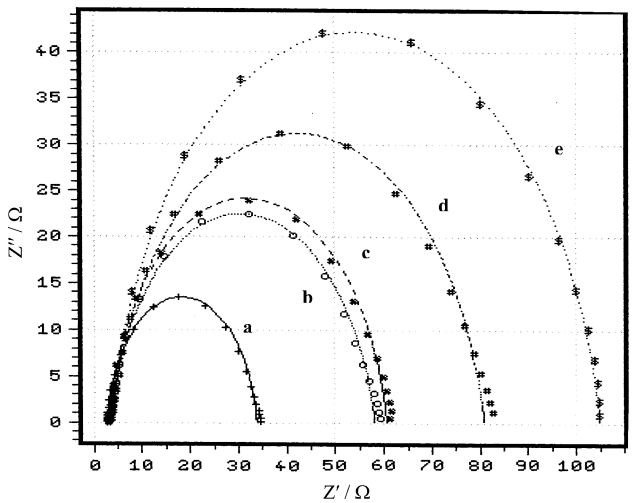


**Fig. 9** The Nyquist plots for carbon steel dissolution in 1 M $H_2SO_4$ in the absence and presence of different concentrations of inhibitor (VI) at 298 K **a**: 0.0 M, **b**: $1 \times 10^{-6}$ M, **c**: $3 \times 10^{-6}$ M, **d**: $7 \times 10^{-6}$ M and **e**: $11 \times 10^{-6}$ M

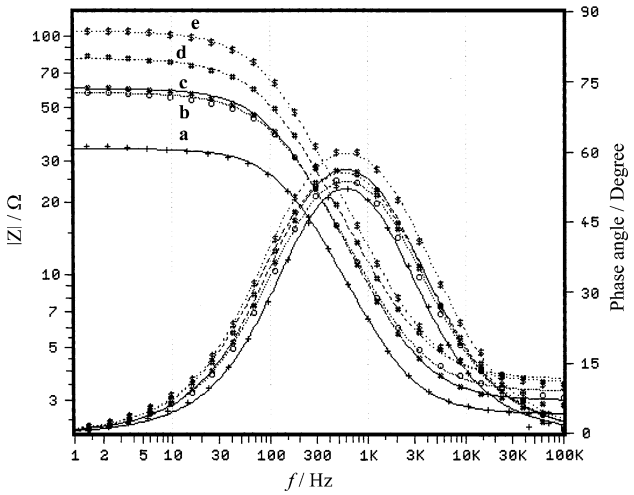


**Fig. 10** The Bode plots for carbon steel dissolution in 1 M $H_2SO_4$ in the absence and presence of different concentrations of inhibitor (VI) at 298 K. **a**: 0.0 M, **b**: $1 \times 10^{-6}$ M, **c**: $3 \times 10^{-6}$ M, **d**: $7 \times 10^{-6}$ M and **e**: $11 \times 10^{-6}$ M

It was observed from the obtained EIS data that $R_{ct}$ increases and $C_{dl}$ decreases with the increasing of inhibitor concentrations. The increase in $R_{ct}$ values, and consequently of inhibition efficiency, may be due to the gradual replacement of water molecules by the adsorption of the inhibitor molecules on the metal surface to form an adherent film on the metal surface and this suggests that the coverage of the metal surface by the film decreases the double layer thickness. Also, this decrease of $C_{dl}$ at the metal/solution interface with increasing the inhibitor concentration can result from a decrease in local dielectric constant which indicates that the inhibitors were adsorbed on the surface at both anodic and cathodic sites [32].

The impedance data confirm the inhibition behavior of the inhibitors obtained with other techniques. From the impedance data (Table 7), we conclude that the value of $R_{ct}$ increases with increase in concentration of the inhibitors and this indicates an increase in the corrosion inhibition efficiency, which is in concord with the weight loss and electrochemical results obtained. In acidic solution, the impedance diagrams show perfect semi-circles (Fig. 9) whose size increases with the concentration of the inhibitor indicating a charge-transfer process mainly controlling the corrosion of steel. In fact, the presence of inhibitors (I–VI) enhances the value of the transfer resistance in acidic solution. Values of double layer capacitance are also brought down to the maximum extent in the presence of inhibitors and decrease in the values of $C_{dl}$ follows the order similar to that obtained for $i_{corr}$ in this study. The decrease in $C_{dl}$ is due to the adsorption of this compound on the metal surface leading to the formation of a film from the acidic solution [33].

**Table 8** Some quantum chemical calculations for the studied inhibitors

| Inhibitors | $-E_{HOMO}$ (eV) | $E_{LUMO}$ (eV) |
|---|---|---|
| I | 3.5807 | 7.8341 |
| II | 3.4807 | 7.8424 |
| III | 3.3763 | 8.0000 |
| IV | 3.3514 | 8.0093 |
| V | 3.1672 | 8.0164 |
| VI | 3.0952 | 8.0253 |

### 3.5 Chemical-quantum calculations

Table 8 shows the energy (in eV) of the highest occupied molecular orbital (HOMO) and the lowest unoccupied molecular orbital (LUMO) for inhibitors. It has been reported that the higher the HOMO energy ($E_{HOMO}$) level of the inhibitor, the greater is the ease of offering electrons to unoccupied d orbital of metallic iron and the greater the inhibition efficiency [34]. The present results show that $E_{HOMO}$ and $E_{LUMO}$ decrease in the order: VI > V > IV > III > II > I which is parallel to the order of inhibition efficiency.

## 4 Corrosion inhibition mechanism

From the previous results of various experimental techniques used, it was concluded that thiadiazole derivatives (I–VI) inhibit the corrosion of C-steel in 1 M $H_2SO_4$ by adsorption at the metal/solution interface. A skeletal representation of the proposed mode of adsorption of studied compounds is shown in Fig. 11 and clearly indicates the active adsorption centers.

The adsorption of the thiadiazole on the metal surface occurs either directly, on the basis of donor acceptor interactions between the $\pi$-electrons of the hetero atoms and the vacant d-orbital of iron surface atoms, or interaction of thiadiazole derivatives with already adsorbed $SO_4^-$ ions [35]. In aqueous acidic solutions thiadiazole derivatives exists either as neutral molecules or in the form of cations. The thiadiazole derivatives may be adsorbed on the metal surface in the form of neutral molecules, involving the displacement of water molecules from the metal surface and sharing of electrons between the nitrogen atoms and metal surface [36]. Heterocyclic nitrogen compounds may also adsorb through electrostatic interactions between the positively charged nitrogen atom and the negatively charged metal surface [37]. It is well known that $SO_4^{2-}$ ions are strongly adsorbed [38] on the metal surface leaving less space available for organic molecules to

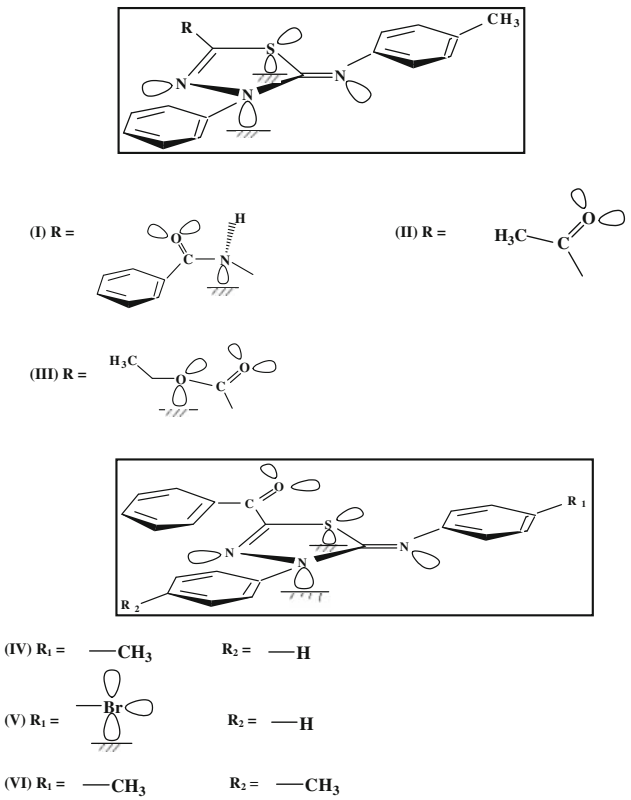


**Fig. 11** Skeletal representation of the proposed adsorption mode of the thiadiazole derivatives on C-steel surface

adsorb. Molecular structure of organic compound is important in synergistic inhibition [39]. The order of the inhibition efficiency of these investigated compounds is as follows: VI > V > VI > III > II > I.

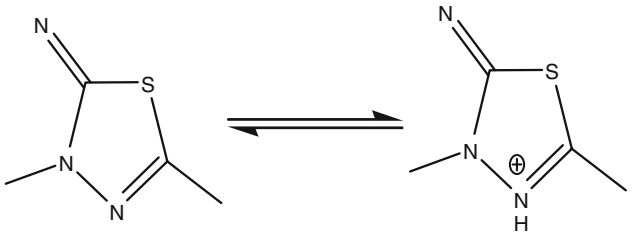

Compound (VI) comes on top of the investigated compounds because of the presence of highly electron releasing para two methyl groups (with Hammett constant $\sigma = -0.17$) [40] which increase the electron density on the active centers and this leads to greater surface overage, thereby giving higher inhibition efficiency. Compound (V), which has the same structure as compound (VI) with the replacement of the two methyl groups by H atom and Br atom [with $\sigma_{Br} = 0.23$ and $\sigma_H = 0.0$] comes next to compound (VI) in the order of % IE. This is due to the operation of a mesomeric effect ($+M$) involving electron pairs on (Br) which act in opposite direction to the inductive effect ($-I$), thus the overall effect of Br atom is to release electrons on the molecule but less than compound (VI). Compound (VI) comes after compound (V) in % IE due to its lesser molecular weight than compound (V). In addition to that, the values of $E_{HOMO}$ decreases in an order runs parallel to increase of % IE obtained which support the order : IV > V > VI.

Compound III is more efficient than compound II due to its higher molecular size. It follows that the ethoxy group is more efficient than the methyl one. From structural organic point of view, both methyl and ethoxy groups have $+R$ effect but the inductive effect is $+I$ For methyl group and $-I$ for ethoxy group. Although the methyl group has $+R$, but its effect is very little as a result of hyperconjugation. In the case of ethoxy group both the effects of $+R$ and $-I$ are larger. Moreover, ethoxy group may add an additional active center to compound (III) and this increases the inhibition efficiency of compound (III) than compound (II). Compound (I) is the least efficient inhibitors in spite of its larger molecular size and it has the same number of adsorption active centers. This can be explained on the basis of the absence of the conjugation between the carbonyl group (–C=O) with azomethine (–N=C–) group in the thiadiazole ring of compounds (I). This leads to lesser surface overage by compound (I) thereby giving lower inhibition efficiency than other tested compounds. In addition to that, the values of $E_{HOMO}$ decreases in an order runs parallel to increase of % IE obtained which support the order: III > II > I.

## 5 Conclusion

(1) The investigated thiadiazole derivatives exhibit inhibiting properties for carbon steel in 1 M $H_2SO_4$.
(2) The % IE increased with the increase in inhibitor concentration. At all concentrations, % IE followed the ranking order: VI > V > IV > III > II > I.
(3) The compounds were inhibitors of the mixed type but the cathode is more polarized than the anode, i.e. they affect both anodic dissolution of carbon steel and hydrogen evolution reactions.
(4) The adsorption of the investigated compounds was found to follow the Langmuir's adsorption isotherm indicating that the inhibition process occurs via adsorption.
(5) The negative value of $\Delta G^{\circ}_{ads}$ obtained from this study indicates that these compounds are strongly spontaneously adsorbed on the carbon steel surface.
(6) A synergistic effect on % IE of a combination of the inhibitors and KSCN, KI and KBr was observed.

(7) The % IE obtained from weight loss, polarization curves, electrochemical impedance spectroscopy measurements and the Stern-Geary equation are in good agreement.

## References


1. Ramesh P, Babu B, Thangavel K (2005) Anti-Corros Methods Mater 52:219
2. Fouda AS, Mostafa HA, Heakal FE, Elewady GY (2005) Corros Sci 47:1988
3. Yurchenko R, Pogrebova L, Pilipenko T, Shubina T (2006) Russian J Appl Chem 79:1100
4. Hossain SA, Almarshad AL (2006) Corros Eng Sci Technol 41:77
5. Abd El-Wahaab S, Gomma G, El-Barradie HY (2007) J Chem Technol Biotechnol 36:435
6. Muralidharan S, Iyer SVK (1997) Anti-Corros Methods Mater 44:100
7. Quraishi MA, Khan MAW, Ajmal M (1996) Anti-Corros Methods Mater 43:5
8. Bentiss F, Traisnel M, Lagrenee M (2001) J Appl Electrochem 31:41
9. Sahin M, Bilgic S (2003) Anti-Corros Methods Mater 50:34
10. Lebrini M, Bentiss F, Vezin H, Lagrenee M (2006) Corros Sci 48:1279
11. Lebrini M, Lagrenee M, Vezin H, Traisnel M, Bentiss F (2007) Corros Sci 49:2254
12. Abd El-Hamid AO, Abd El-Wahab BAM, Al-Atom AA (2004) Phosphorus Sulfur Silicon Relat Elem 179:601
13. Tsuru T, Haruyama S, Boshoku G (1978) J Jpn Soc Corros Eng 27:573
14. Gomma GK (1998) Mater Chem Phys 55:243
15. Larabi L, Harek Y, Traisnel M, Mansri A (2004) J Appl Electrochem 34:833
16. Aramaki K, Hagiwara M, Nishihara H (1987) Corros Sci 27:487
17. Ochoa N, Moran F, Pebere N (2004) J Appl Electrochem 34:487
18. Bentiss F, Bouanis M, Mernar B, Traisnel M, Lagrenee M (2002) J Appl Electrochem 32:671
19. Aramaki K, Hackerman N (1969) J Electrochem Soc 116:568
20. Bereket G, Yurt A, Turk H (2003) Anti-Corros Methods Mater 50:422
21. Bensajjay F, Alehyen S, El-Achouri M, Kertit S (2003) Anti-Corros Methods Mater 50:402
22. Duan SZ, Tao YL (1990) Interface chemistry. Higher Education Press, Beijing, 124 pp
23. Abd El-Rehim SS, Refaey SAM, Taha F, Saleh MB, Ahmed RA (2001) J Appl Electrochem 31:429
24. Al-Neami KK, Mohamed AK, Kenawy IM, Fouda AS (1995) Monatsh Chem 126:369
25. Haladky K, Collow L, Dawson J (1980) Br Corros J 15:20
26. Abd El-Rehim SS, Ibrahim MAM, Khaled KF (1999) J Appl Electrochem 29:593
27. Fouda AS, Al-Sarawy AA, Radwan MS (2006) Ann Chim 96:85
28. Mohamed A, Mostafa HA, El-Awady GY, Fouda AS (2000) Port Electrochim Acta 18:99
29. El-Ouafi A, Hammouti B, Oudda H, Kerit S, Touzani R, Ramdani A (2002) Anti-Corros Methods Mater 49:199
30. Mansfeld F, Kendig MW, Tsai S (1982) Corrosion 38:570
31. Mansfeld F (1990) Eletrochim Acta 35:1533
32. McCafferty E, Hackerman N (1972) J Electrochem Soc 119:146
33. Bentiss F, Largrenee M, Traisenl M, Hornez JC (1999) Corros Sci 41:789
34. Ogretir C, Mihci B, Bereket G (1999) J Mol Struct 488:223
35. Hackerman N, Snavely E Jr, Payne JS Jr (1966) Electrochem Soc 113:677
36. Hackerman N, Makrides AC (1955) J Phys Chem 59:707
37. Mann CA (1936) Trans Elctrochem Soc 69:105
38. Murakawa TM, Hackerman N (1964) Corros Sci 4:387
39. Tsuru T, Haruyama S, Gijutsu B (1978) J Jpn Soc Corros Eng 27:573
40. Hammett LP (1940) Physical organic chemistry. McGraw-Hill Book Co., NY